PERIODICA POLYTECHNICA SER. TRANSP. ENG. VOL. 32, NO. 1–2, PP. 91–112 (2004)

HEAT TREATMENT INDUCED MECHANICAL AND ELECTRICAL PROPERTY CHANGES IN FE_{40} NI_{40} B_{14} SI_6 GLASSY ALLOYS USED AS SEASONAL HEATING ELEMENTS IN TRANSPORTATION ENGINEERING

Csaba GULYÁS and Antal LOVAS

Department of Vehicle Manufacturing and Repairing
Budapest University of Technology and Economics
H–1521 Budapest, Hungary

Received: Sept. 30, 2003

Abstract

$Fe_{40}Ni_{40}B_{14}Si_6$ amorphous alloy owns average soft magnetic properties but its mechanical and electrical characteristics are impressive. We investigated whether it can be used as heating element in resistivity heating based on its high electrical resistivity and mechanical flexibility. We found that these property changes during long time heat treatments are not significant, allowing us to propose this alloy for this new application. Beside this technically important result we found that the microhardness, tensile strength and flexibility change during the structural relaxation in a different way as it is described in the relevant literature. We try to give an explanation of this unusual behaviour. This can contribute to the general understanding of structural relaxation in the metallic glassy state.

Keywords: amorphous alloy, reversible relaxation, metallic glass, electrical resistivity, hardness, flow and fracture, electrical heating.

1. Introduction

Amorphous alloys are members of a relatively new class of metallic materials, which were developed three decades ago [1]. Their development is the consequence of the increasing interest in the non-equilibrium alloys such as martensitic high strength steels of high hardness produced by high cooling rates avoiding the carbon diffusion in the gamma-Fe lattice. When the cooling rate of a multicomponent melt exceeds 10^2 K/s, a new non-crystalline solid metallic phase can appear. It is called amorphous alloy because of the lack of 'long range' crystalline structure. Although it was first produced already in 1960, there are many new properties of this group of alloys that haven't been completely discovered and understood yet.

Amorphous alloys have totally different characteristics compared with crystalline metals. Their special and sometimes conflicting properties allow us using them in new or old application fields, mainly in connection with their high quality soft-magnetic properties. In this paper a new type of application will be presented, based on a special type of glassy alloy. Our aim is to manage to use the Fe-Ni-based metallic glasses as heating element in seasonal defrosting systems.

The main purpose of our experimental work is the partial replacement of old and nature-polluting defrosting tools by new, more effective and less pollutant systems. According to this principle, the most suitable way of the elimination of slippery caused by the ice and snow deposition in stops of public transport vehicles and on sidewalks is the electrical heating. Electricity can be produced from renewable energy resources such as wind, water or sun power. The heat needed for defrosting arises directly underneath the heated surfaces, which increases the efficiency. The presented electrical systems are capable of operating in lower temperature range than the traditional methods in which a mixture of sand and salt is spread on snowed or iced surfaces. A schematic view of a possible heating arrangement is illustrated in *Fig. 1.*

The main physical and technical requirements for the heating element in outdoor application are: it should have high specific resistance together with small temperature dependence (α) to ensure a nearly constant heating performance in wide temperature range. The applied alloy should have high corrosion resistance and ability to operate at temperatures, up to 250 °C. It is also necessary that the alloy can endure the mechanical stresses during cementation of the surrounding concrete and the possible thermal dilatation. Another important benefit arises from the solderability, which enables easier construction and tailoring the heating circle for a given purpose.

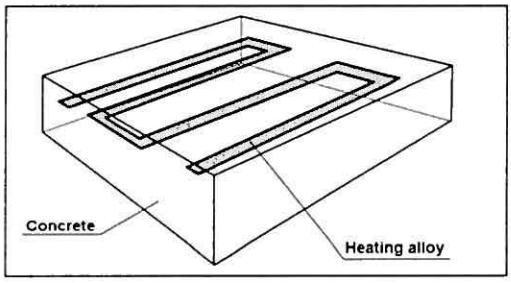

Fig. 1. Possible heating arrangement

In general, many of the well-known metallic glasses can be characterised by all of the listed properties within a strict temperature range. Its origin is the thermal stability of glassy state and the impairment of the embedding concrete at high working temperature such as 250 °C. As the temperature of amorphous/crystalline transformation is approached, irreversible property changes occur in the metallic glasses. The limit of the operating temperature is the crystallisation onset, at which the described favourable properties are breaking down. Avoiding the undesirable crystallisation, a temperature switch is applied based on the adjustable amorphous Curie temperature (T_c), which is well below that of the crystallisation in this system. On this basis a suitable electronic circuit was constructed that can break the heating circle avoiding the local overheating. A more detailed description can be found in [5].

The main topics of this article are the:

- description of the important application oriented properties of $Fe_{40}Ni_{40}B_{14}Si_6$ metallic glass
- theoretical background of the relaxation process taking place in the operating temperature range of the application and its effect on the mechanical and electrical properties of amorphous alloy to be applied
- the evolution of tensile strength, hardness, ductility and temperature coefficient of resistivity of $Fe_{40}Ni_{40}B_{14}Si_6$ metallic glass during short and long time annealing

2. Analysis of Properties of Glassy Alloys

2.1. Production of Metallic Glasses

Nowadays we can produce amorphous alloys in various ways. The most common ones (described later on) result in the so-called 'metallic glass' formation. The different naming hints to the production method. Glassy alloys are rapidly quenched from a melt with a quenching rate of $10^2 - 10^{11}$ K/s depending on the alloy-composition. To achieve such high cooling rates effective heat sink is necessary with good contact to the melt.

Depending on the connection between the melt and the heat sink and the desired geometry, three main production classes can be distinguished: 'spray methods', 'chill methods' and 'weld methods', however 'weld methods' are not suitable for producing separated metallic-glass parts.

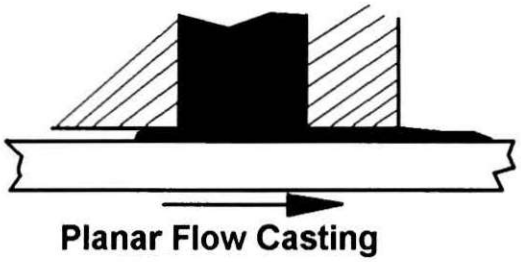

Fig. 2. Planar Flow Casting, typical method of chill casting [2]

While spray methods are used to fragment the melt into droplets prior to quenching, chill methods are capable to produce continuous solid parts like bands or wires. The schematic illustration of the ribbon formation process (chill casting) can be seen in *Fig. 2*. Weld methods are the best from the view point of heat contact, because the frozen melt to be amorphised will be melted directly on the surface of the heat sink. This is the main drawback of the method, though, except a surface treatment is the goal.

2.2. *General Comparison of Amorphous and Crystalline Metals and Alloys*

Alloys with amorphous structure can combine the malleability, conductivity and magnetic softness of metals with the high mechanical hardness and corrosion resistance. For other materials, such properties depend on the structure as defined by electronic and atomic interactions and arrangements and by other macroscopic features such as cracks, long-range compositional variations, inclusions, cavities or surface steps where present. In this aspect the mechanical properties are especially interesting. They combine ductile behaviour in bending, shear and compression with high flow stress and hardness with a fracture-stress ~E/50 that approaches the theoretical limit. Such behaviour contrasts sharply on the one hand with the brittleness and low fracture-stress of ceramic oxide glasses and on the other hand with the relatively low strengths associated with ductile behaviour in crystalline metals.

The lack of atomic order shows up in the difference of electrical properties of amorphous and crystalline metals. Metallic glasses have in general high electrical resistivity with a negligible temperature coefficient. The amorphous state resembles more the electrical properties obtained by measuring the properties of a melt [1].

From chemical point of view amorphous alloys often exhibit high corrosion resistance partially as a consequence of defect free structure without grain boundaries, dislocations and stacking faults. However, in spite of their diffusion-less formation macroscopic segregation can occur [3]. As a consequence, amorphous alloys have nearly the ideal structure for high corrosion resistance even if the composition is inhomogeneous. The large fraction of metalloids necessary for easy formation of amorphous structure should also increase corrosion ability in certain glasses. In spite of the conflicting effects arising from structural and compositional origin, amorphous alloys show high corrosion resistance possibly caused by a thin passive layer surrounding the surface [4].

2.3. *Characterisation of $Fe_{40}Ni_{40}B_{14}Si_6$ Glassy Alloy Applied as Resistance Heating Element*

This kind of amorphous alloy was never studied very intensively because it does not exhibit superior soft magnetic properties. As the requirement of producing wide amorphous bands became more and more important, Fe–B based metal-metalloid systems were investigated more frequently. Although the Ni addition (partial replacement of Fe by Ni) is unfavourable from the point of view of soft magnetic properties the glass forming ability (GFA) is higher.

Hence, the $Fe_{40}Ni_{40}B_{14}Si_6$ composition suits well for using as heating element partially due to high glass forming ability and high specific resistance characteristic of glassy state. The high electrical resistivity of glassy state, arising form the absence of crystalline periodicity is similar to that of the appropriate liquid state. It is $1.4529 \cdot 10^{-4}$ Ω cm in as quenched (a.q.) state, which is about one magnitude

higher than that of copper. This high resistivity is advantageous in resistance heating making possible to reduce the necessary length of heating wire or band while producing the same heating power. The benefit of low temperature coefficient of resistivity is obvious in the power regulation of real applications.

The mechanical properties of the applied $Fe_{40}Ni_{40}B_{14}Si_6$ glass are also impressive. The tensile strength is about 2500 N/mm^2, micro hardness is 1150 HV in a. q. state (measured on samples of 12 mm width and $\sim$ 30 μm thickness). The flexibility was characterised by bending tests (bending number, n is around 800). These data confirm that high flexibility is combined with high tensile strength and hardness in this type of glassy alloys.

As a consequence of high Ni content, the GFA is high enough for the production of ribbons in wide variability of the width and thickness. The thermal stability is also remarkable allowing operating temperatures up to 250 °C . Consequently, the soldering (short time heating beyond 250 °C) can also be applied without any risk of damages.

Finally, the ribbon shape has an advantageous geometrical form (large surface) from the point of view of efficient heat transport between the heating element and the embedding concrete.

Based on the outlined characteristics, the $Fe_{40}Ni_{40}B_{14}Si_6$ metallic glass seems to suit good for heating purposes. The expectable lifetime is important from the point of view of real applications. Therefore, isothermal heat treatments at various temperatures were carried out in order to get information about how the electrical and mechanical properties would change after operating several hours at different temperatures. Long term operating below the T_{cr} results in structural relaxation of the glassy state. To understand the property changes during the structural relaxation represented by heat treatments, a short summary of the theoretical background of the structural relaxation will be given in the next paragraph.

3. Relaxation

Structural relaxation in metallic glasses is a thermally activated process, during which the frozen-in melt structure reaches an internal equilibrium via short-range atomic arrangement [6]. As a result, many physical properties (electric, magnetic and mechanical) change in the glassy state.

The interpretation of the relaxation phenomenon, especially the elimination of macroscopic stresses, is relatively simple in the case of crystalline metals and alloys. With increasing temperature, the atomic mobility raises and the macroscopic stress together with the microscopic segregation, vacancies and dislocations will be annealed out, while the long-range crystalline periodicity remains intact.

In contrast, the relaxation of the amorphous structures is much more complex. Property changes can not be explained by altering of the overall stress state (annealing out of point defects and dislocations), because they resemble more a frozen-in melt structure. Moreover, amorphous structure is not in an equilibrium state even after the structural relaxation.

3.1. Relaxation Kinetic and Micro Mechanism

Isothermal relaxation kinetic of as-quenched metallic glasses below and near T_g seems to obey a log (t) law during equilibration. However, in case of stress relief and magnetic ageing performed well below T_g, the kinetics can be described as a first order reaction. The same happens to samples being preconditioned or stabilised by heat treatments.

The analysis of thermograms of certain metallic glasses points to the complexity of relaxation processes in amorphous structures consisting of an irreversible and a reversible part. The reversible part is believed to arise from short-range localised structural relaxation in a stable matrix (chemical short range ordering, CSRO). The irreversible part is thought to be due to results from the annihilation of defects leading to the reduction of free volume (topological short range ordering, TSRO). This is a medium range, co-operative structural relaxation, involving only a portion of the glassy material. Another component of irreversible relaxation is the expansion of the stabilised atomic regions over the whole system caused by long-time annealing approaching the glass forming temperature (T_g) [6].

According to the recent relaxation theories the reversible part of the structural changes leading to reversible property altering can be well explained by a thermodynamic model. In this aspect, the atoms of an amorphous structure can be regarded energetically as participants of a two-level system (TLS) with a splitting and an activation energy parameter. Reversible property changes take place when the splitting is greater than zero. In this case, with increasing temperatures, atoms can overcome the activation energy between the two energy levels and gather nearly equally both in the higher and the lower state. If the temperature falls, atoms can get back into the lower energy-state until their energy is higher then the activation energy threshold. Now, if the number of atoms at an energy level is different compared with that of the starting stage, physical properties also differ. According to [7] the number of TLS and their activation energy can be calculated, which gives numerical values for the description of reversible relaxation.

3.2. Property Changes During Relaxation

According to available data, relaxation processes consist of a low temperature $T \ll T_g$ and a high temperature part, near T_g. This is clear by measuring macroscopic properties, e.g. volume, enthalpy and Young's modulus, structural sensitive properties, e.g. microhardness, soft magnetic properties and semimicroscopic properties, e.g. electrical resistivity and Curie temperature (T_c^{am}). In the following only the mechanical and electrical property changes will be treated in detail.

3.2.1. Mechanical Properties

The mechanical properties of a metal can be characterised basically by hardness, yield strength and ductility measurements. As discussed above, the appropriate properties of crystalline and amorphous alloys differ strongly.

In crystalline state the altering of mechanical properties of metals upon annealing is a complex process. It depends on the actual stress-state and on the composition. During annealing the disordered structure, arising from the mechanical processing (plastic deformation), usually forms a defect free lattice with lower hardness and high plasticity. In multi-component alloy, however, the heat treatment can result even in a hardness increase due to the precipitation of a second phase. The resulting hardness and plasticity depends on the individual contribution of these processes.

Amorphous alloys exhibit only negligible work hardening. Due to the compositional effect, there is also solution hardening but it is masked by the effect caused by the atomic disorder. Precipitation hardening is absent because of the single-phase nature of metallic glasses.

In spite of the similarities between crystalline and glassy metallic state the hardness and brittleness of amorphous alloys show always an increasing tendency during annealing.

3.2.2. Hardness

The hardness of a material is its resistance against indentation. In the case of crystalline metals and alloys, the hardness (HV) depends on several factors (composition, type of chemical bonds, crystalline orientation allotropy, grain size, stress state, etc [8]). The simple linear compositional dependence of HV in metallic glasses, which leads to a nearly linear dependence of the HV on the outer electron concentration per atom (e/a) is the consequence of single phase nature of the glassy state, leading to the predominant role of the composition. However, the significance of the quenched-in stresses and the thermal history was also pointed out in the mechanical properties of Fe-based glasses [9].

The alloying effect, i.e. the role of transition metal TM replacement of the Fe host metal can be interpreted qualitatively on the basis of Hume Rothary rules. It has been found that atomic size and electron-negativity difference between the transition elements have only slight influence on the hardness in these alloys. On the contrary, the change in e/a due to alloying has a dominant effect in this respect [10]. It is also verified that the increasing sp character in the average bonding state (increasing concentration of metalloids) raises the covalent character, hence the hardness of the glass will be increased [9].

It is a qualitative correlation between the HV and thermal stability that was first recognised in crystalline metals. According to this, HV can be estimated by the melting point, molar volume, molar weight and measuring temperature [8].

However, T_m is an average temperature in most cases. The thermal stability of a multi-component crystalline alloy can only be characterised by a single T_m, at single-phase or at the eutectic compositions. This shows that binding energy is not necessarily identical in the whole structure. The same is valid for the crystallisation mechanisms of amorphous alloys around T_g at which the glassy state turns into the supercooled liquid state. This process requires high atomic diffusion just as by the melting of a crystalline metal. From this point of view T_g and T_m are comparable. In addition, T_g must be an average value because crystallisation of amorphous alloys can also occur in more than one stages depending on the number of metalloid components. Its reason is a strong clasterisation arising from the local concentration of the compounds.

The effect of the cooling rate does also contribute to the evolution of HV in which a 'self annealing' effect is coupled with the solidification process. As the average cooling rate is lowered the resulting (thicker) ribbons will be more relaxed, exhibiting higher hardness.

3.2.3. Flow and Fracture [12]

The reaction of solid materials upon mechanical stresses consists of a reversible and an irreversible portion. While in crystalline substances elasticity depends on the crystalline orientation and grain structure, metallic glasses can be considered elastically isotropic, so their stress/train response is characterised by Poisson number and shear modulus, which is about 20–30% smaller than that in crystalline form.

Anelasticity (plasticity) is connected with generally thermally activated atomic movements and lattice-defects.

In general, metallic glasses can be deformed plastically relatively well, up to 50% without fracture, in contrast with covalent glasses, such as SiO_2 glass. The plastic response of metallic glasses exhibits similarities to crystalline alloys, but significant deviations do also occur. The complexity of the anelastic deformation in the glassy-state shows up in the collective existence of a homogeneous and an inhomogeneous flow. While during the homogeneous flow each volume element contributes to the global strain, plastic deformation takes place in highly localised slip bands.

Homogeneous flow, opposite to inhomogeneous ones, proceeds at higher temperatures near T_g and at lower stress-levels. This behaviour can be studied in creep and stress relaxation.

The creeping of amorphous and crystalline alloys is especially different. In the first, transient creep stage crystalline metals exhibit a firm hardening, while the HV of amorphous alloys remains constant. It points obviously to the absence of work and deformation hardening in glassy state caused by the obstructive effect of the increasing dislocation density on their mobility. One may think its explanation is that amorphous structures are already in a completely disordered state, which is approached by the increasing degree of deformation in the crystalline alloys.

Analysing the steady state creep after the transient stage gives the result, that flow is here controlled by diffusion mechanisms similar to that occurring in the liquid state.

The last part of creeping, immediately before fraction, is also different in crystalline and amorphous alloys. In contrast to crystalline solids, accelerating creep does not appear in metallic glasses prior to fracture. The fracture takes place generally just at which may be the onset of the accelerating stage.

There are basically two theoretical explanations how the homogeneous deformation can take place in metallic glasses. The atomic movements, as the basic control of the diffusion, are possible due to the existence of the free volume in the neighbourhood of an atom representing a lower energy position. Upon applying an external force, atoms will move in direction of the induced stress with higher probability than in any other orientation [13]. According to the entropy model of plastic flow [14] atom transport in the glassy state takes place by co-operative atomic rearrangement characterised by a viscosity depending on the ratio of $\mathrm{d}G/(T\,S_c)\cdot \mathrm{d}G$ is the smallest energy necessary for a given atomic rearrangement and S_c is the configuration entropy. According to the theory S_c vanishes in a second order phase transition at a temperature lower than the glass-transition (one). In this case viscosity scales only with the activation energy $\mathrm{d}G$.

Inhomogeneous flow may occur in metallic glasses at higher stresses (10^{-2} GPa) despite of temperatures well below T_g. Deformation appears only in narrow shear bands with a typical length of 1 μm. The shear strain can here exceed 10%, while other regions remain practically unchanged. Due to the appearance of the shear-bands macroscopic ductility and local chemical resistivity are lower.

3.2.4. Tension and Fatigue, Inhomogeneous Flow

Yield-stress of metallic glasses is difficult to estimate due to small extent of the plastic deformation. Even the 0.2% plastic elongation is rarely achieved. However, a firm residual plastic deformation can be observed on the hysteresis loops upon unloading and reloading the samples. The ultimate tensile strength is more definite, and is easy to measure. The highly localised shear-bands appear always in 45 ° planes, according to Mohr–Tresca flow criterion, both in length and cross directions.

The behaviour of metallic glasses exposed to cyclic loading is similar to that of crystalline metals. However, the tendencies upon annealing at increasing temperatures contrast to the softening and higher cycle numbers of crystalline metals. The shear bands appear also here after the fraction.

3.2.5. Electrical Properties

The increased scattering of electrons by the disordered structure and mixed population of atomic species in a metallic glass gives rise to high electrical resistivity,

typically 100–300 μOhm-cm at room temperature, which is 2 or 3 times higher than that of the same composition in crystalline form. This property is very advantageous for using them as electrical heating elements.

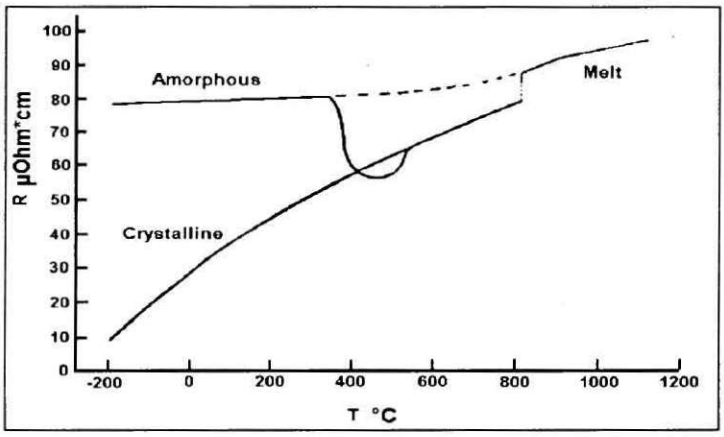

Fig. 3. Resistivity of amorphous, crystalline state and melt [15]

Like in the crystalline metals and alloys, resistivity decreases with decreasing temperature but with a relatively small temperature coefficient of resistivity (TCR), until distinct minimum in resistivity is reached at sufficiently low temperatures. Above this minimum the resistivity appears to extrapolate smoothly to that of the liquid alloy entirely consistent with the concept of the state of metallic glass as a super-cooled liquid and drops sharply on crystallisation, see *Fig. 3* [1].

The occurrence of a resistance minimum in low temperature range, well below a ferromagnetic transition is unusual and has rarely been observed in crystalline alloys. In amorphous alloys containing large amount of ferromagnetic, paramagnetic and anti-ferromagnetic elements as in the case of our material (Fe, Ni, Si, B, etc.), resistivity has a minimum in the temperature range 5 K to 300 K. Below this temperature resistivity increases approximately logarithmically with decreasing temperature [16]. Several theories have been developed to explain the negative TCR observed in these glasses, but non of them can give a complete explanation of this phenomenon. The recent studies suggest a magnetic origin of this special $\rho(T)$ dependence, which can be explained in terms of a variation on the normal Kondo scattering mechanism [16].

4. Experiments

The technically important mechanical properties like ductile to brittle transition (which can be easily characterized by the bending number n), hardness (HV) and tensile strength (σ), are also influenced by the quenching conditions [17]. Therefore,

all of the measurements have been performed on the $Fe_{40}Ni_{40}B_{14}Si_6$ ribbons arising from the same production charge. Ribbon thickness is 37 μm and the width is 11.5 mm respectively. Isothermal heat treatments were carried out on 200 mm long pieces, at 473 K ($\pm$3 °C) in atmospheric circumstances using commercial box furnace. The samples were placed between two polished sheet-tiles in the furnace during the heat treatment period, avoiding any indefinite deformations. Hanemann type of microhardness tester was applied for the hardness characterization, with the typical loading of 40, 100 g. INSTRON 1195 equipment was used for the tensile strength measurements. It is well known that fixing of thin, ribbon-shaped samples in tensile strength measurements is difficult [18]. Thereby special care was taken during the preparation of probes, avoiding the indefinite slip in the jaw. Ribbons were placed between two Bakelite sheets using appropriate adhesive (see insert in *Fig. 4*). A simple home-made bending tester was applied to follow the change of ductile to brittle transformation (applied load was $\sim$ 40 N, bending angle was 90° see insert in *Fig. 6*). Because significant fluctuation was observed in the investigated properties, especially during the early period of heat treatments a new series of critical measurements was performed.

In this case, the heat treatments were carried out at 150 °C, 200 °C, 250 °C, 300 °C and at 350 °C, respectively. The new series of HV measurements were performed with a load of 40 p. The duration of the heat treatments was 1, 2, 4, 6, 12 and 24 hours at each temperature. The HV measurements were continuously repeated after each heat treatment at room temperature, on the same sample over a 6 hours time-period in every 0.5, 1.5, 3, 6 hours. In addition, one of the samples was cooled subsequently to liquid N_2 temperature (-196 °C) for 6 hours in order to complete all possible structural changes. After this 'overcooling' the HV of these samples was measured again. All of the presented results refer to experiments carried out on samples of $\sim$ 30 μm thickness. The HV value of a sample was calculated as the average of 12 indentations being taken at every measurement. The scattering was evaluated by using the method of standard deviation.

The TCR of the same samples was measured in a thermally isolated but, open vacuum bottle. It was first filled with liquid N_2 and the sample holder was placed into. In this way a reliable slow warming-up was ensured, during which the temperature and the sample resistivity were measured by a Keithly nano-voltmeter. The temperature range was form -192 °C to $+5$ °C, and the average warming-up rate was 1.5 ° C/min.

5. Long Time Heat Treatments at 200 °C

5.1. Tensile Strength

Tensile strength slightly increases with the time of isothermal heat treatment as *Fig. 4* shows. The measurements do show considerable scattering, which is thought primarily to be the consequence of uncertainties in sample fixing (small deviation

from the co-axial fixing can result in a considerable lowering in the measured strength values). Consequently, for the construction of *Fig. 4* the values $R_{m\,\max}$ are used from the parallel measurements only. A photomicrograph of the fractured cross-section was taken after each heat-treatment. One can see here the slip bands typical for glassy alloys (white lines), where the plastic deformation predominantly occur. Although the pictures were taken of samples being heat-treated at various circumstances no definite trend of the fracture surfaces can be observed as a function of the duration of the annealing. However, the morphology of the fractured cross sections differs at the quenched and heat treated samples. A grain boundary-like net and layer structure appear after certain stage of heat treatment.

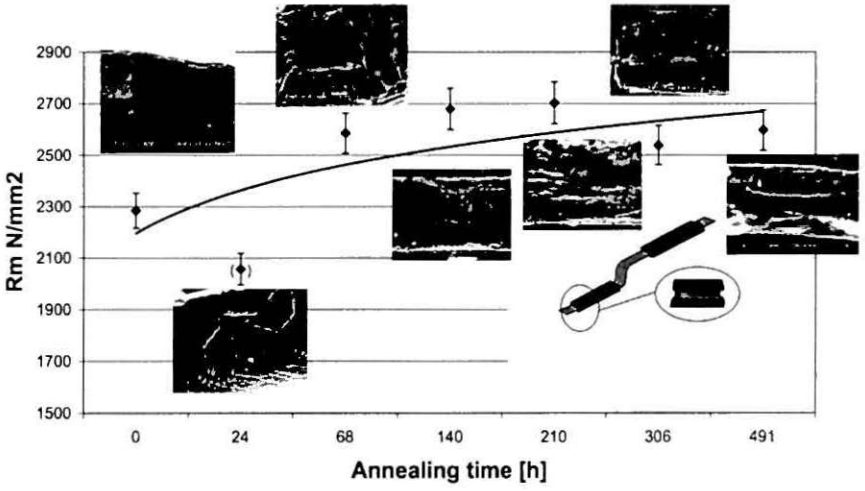

Fig. 4. Tensile strength R_m of $Fe_{40}Ni_{40}Si_6B_{14}$ glassy ribbons as a function of aging time carried out at 200 °C. The morphology of the fractured surfaces is illustrated by the scanning electron micrographs

5.2. Microhardness

In *Fig. 5* the change in microhardness is plotted versus the time of heat treatment, carried out also at 200 °C. The HV increases monotonically versus t_{anneal}. Note, that deviation from the monotonic change (temporal maximum or minimum) can be also observed. The appearance of temporal HV maximums depends highly on the temperature of the applied heat treatment. From this scattering the co-existence of various hardening mechanisms cannot be excluded even in the glassy state. It is remarkable, that a singularity in HV seems to appear also (short heat treatment times at around 24 h).

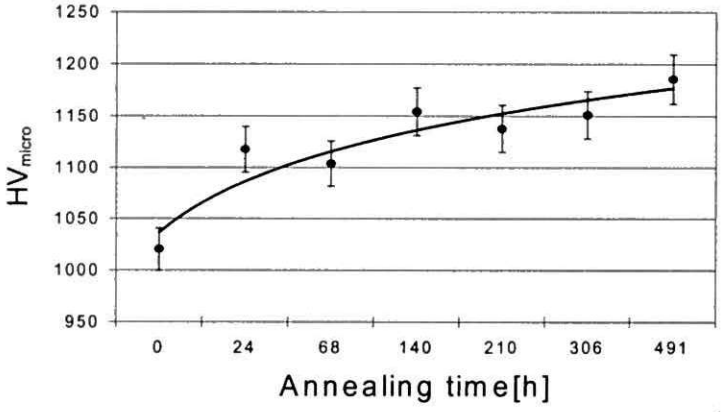

Fig. 5. The change of microhardness with the time of isothermal heat treatments at 200 °C

5.3. Ductility Measurement

During joule heating of ribbons the temperature is around 150–180 °C in the bulk glass. As a consequence of balance between the continuous heat evolution and the heat flow into the embedding media, the overall temperature at the surface of the heating element is around 140–160 °C [19]. Though the actual temperature is low, related to the T_{cryst} of the glass, a substantial structural relaxation occurs during this long time operating period causing significant change also in the flexibility. This is an especially important parameter when the difference in the thermal expansion of the heating element and the embedding material are considered.

The abrupt decrease of bending number versus the duration of heat treatment, shown in *Fig. 6*, hints to the dominant role of rapid, diffusion-less process in which the covalent bonding character is strengthened, increasing the brittleness of the glassy state. Note that brittleness increases further during the crystallization in transition metal-metalloid glasses. However, it is not visible in *Fig. 6*, as there is no detectable crystalline portion in the glass after the applied heat treatment.

5.4. Conclusion

Considerable structural relaxation is manifested in all measured mechanical properties during the heat treatments of $Fe_{40}Ni_{40}Si_6B_{14}$ glassy ribbons at 200 °C while all of the measured properties tend to reach a saturation value versus the annealing time.

The mean trend in all property changes is in agreement with the expectable structural relaxation and earlier results in the literature. However, there is no expla-

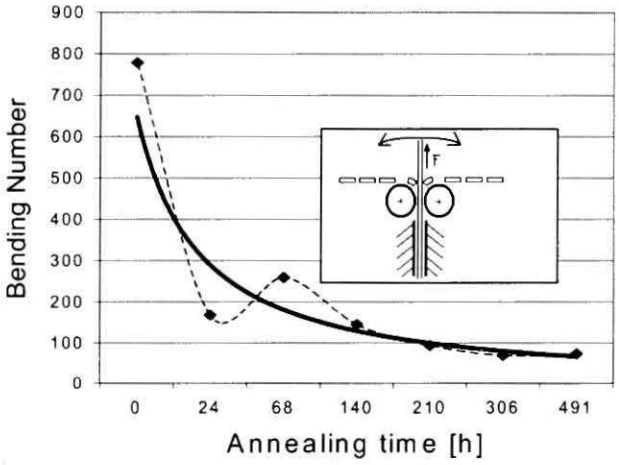

Fig. 6. The time dependence of bending number on the time of isothermal heat treatments at 200 °C

nation of the experienced maximums or minimums at short heat treatment periods. To get closer to the reason of this phenomenon we performed a new series of critical measurements. The results are presented in the following.

6. Short Time Heat Treatments at Various Temperatures

6.1. Microhardness

In agreement with the previous results the HV increases with increasing time and temperature of heat treatments. The fluctuation of HV values in the early period of heat treatments is confirmed by the new series of measurements, as it is obvious from the *Fig. 7*.

The HV(t_a) curves exhibit minimum in the first period of the heat treatment, at around 2h annealing. This shifts to shorter times as T_m is raised. On the other hand, an explicit maximum can be seen in each curve. The values of these maximums increase up to 300 °C and turns back in decreasing for the curve referring to 350 °C. Comparing the HV(t_a) curves, we can notice that every figure begins with a softening. This softening phenomenon appears after short annealing times at 250 °C and 300 °C and stretches for as longer as higher T_a is. Similar trends can be observed in the T_c^{am} of these samples. T_c^{am} increases with the annealing temperature and time and then drops when 350 °C is exceeded [20]. It is also worth to notice that the samples heat treated at 350 °C for 24 h contain already a detectable crystalline fraction.

The samples that were heat-treated at 150 °C and 200 °C, exhibit unusual behaviour. The HV for samples annealed at 150 °C is lower compared with that of the a.q. state ones including also HV maximums which come up also here. At 200 °C, the maximum appears later referring to the other curves and its HV sinks below the HV of the a. q. state due to softening. Furthermore, the HV increases generally with the annealing time expect the samples heat treated at 300 °C and 350 °C. Their HV values after an annealing time of 24 hours are lower than the maximums and nearly equal to that of the a.q. state [21].

To sum up, our results show that the general conception about monotone HV increase with t_{an} and T_{an} has limited validity only. The HV altering in our case is not monotone at all, however, the altering is tendentiously growing at $T_{an} < 300$ °C.

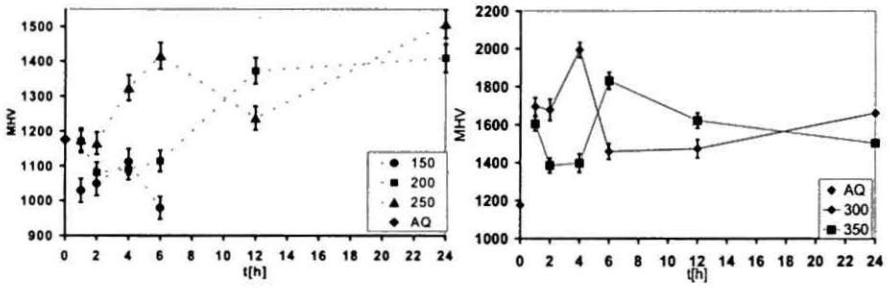

Fig. 7. The dependence of HV on the time of isotherm heat treatments at various temperatures. Deviation is shown in 1 : 10 size

6.2. *Flexibility*

The flexibility was measured using bending tests. Although this method is less exact than the HV measurement (due to the large scattering, up to 50%, showing up in the raw data), the average values (*Fig. 8*) represent such tendencies, which are qualitatively supported by the HV measurements. The bending number (n) is surprisingly high after heat treatments at 200 °C, which is reasonable, considering the inverse relation between the HV and mechanical flexibility. It is remarkable that such kind of softening tendency with simultaneously increasing flexural strength at a certain period of structural relaxation can be rarely found in the literature.

6.3. *Analysis of HV Scattering*

As it can be observed in *Fig. 7* by the hardness values, the measurements are loaded by a large deviation. The scattering may arise from technical artifact (stresses in-

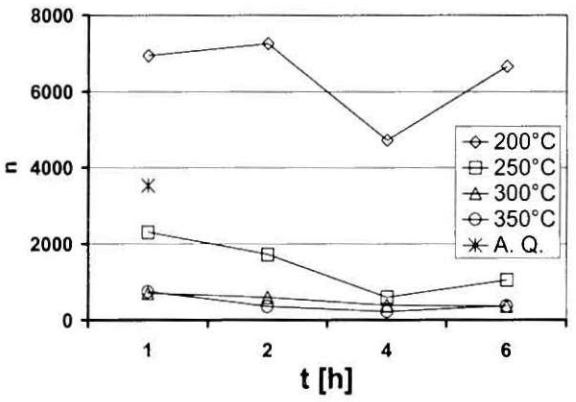

Fig. 8. Evolution of the values of bending number (n) during isotherm annealing at various temperatures

duced by fixing the sample on the substrate) or from the so called 'thickness effect', caused by the comparable value of ribbon thickness to the indentation depth in the investigated samples. Therefore, the proposed load-to-thickness ratio was controlled in our experimental conditions. Ref. to [18], the diagonal of the indentation should not be longer than 70% of the sample thickness. At a load of 40 p we obtained an indentation diagonal 7.8 μm . The thickness of our samples was $\sim$ 30 μm so we did not exceeded its 70% (21 μm). Another source of the large HV scattering can be the indefinite stress change in the sample during room temperature resting subsequently a certain type of heat treatment.

In order to get additional information about the HV changes during the resting time, the calculated deviation of the HV values has been compared with that in the as quenched state as it is demonstrated in *Fig. 9.* The scattering of the HV data is considerable. As we can see, the deviation is the smallest in the a. q. state. The HV values of the samples measured immediately subsequent to a heat treatment, show higher deviation just as after 3 and 6 hours.

Between 0 and 3 hours we found a small scattering of HV data similar to that of the a.q. state and the samples being cooled to liquid N_2 temperature for 6 hours. One can conclude that the standard deviation is obviously a function of the resting time at room temperature. Consequently the scattering has a physical origin rather than the 'insufficient reproducibility' of the HV measurement.

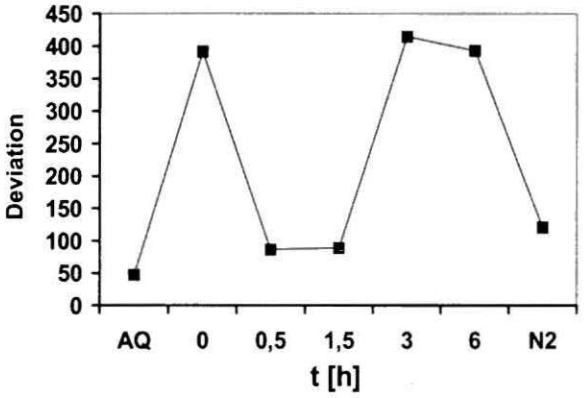

Fig. 9. The change of the average standard deviation of the HV evolution during the resting time at room temperature and measured on samples cooled in

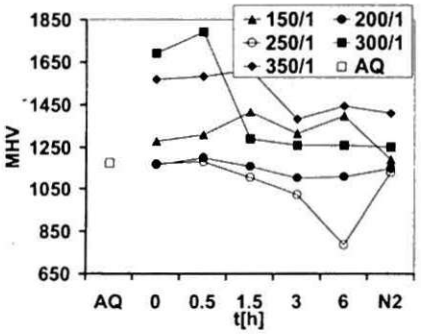

Fig. 10.a. The change of HV during the resting time after heat treatment for 1 hour at various temperatures

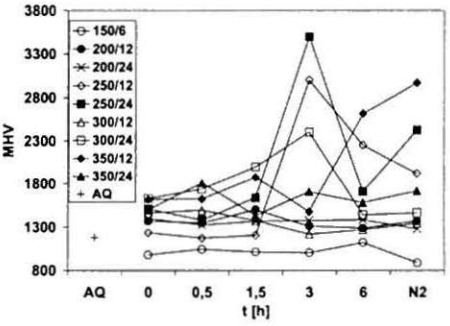

Fig. 10.b. The change of HV during the resting time after treatment for 6, 12, 24 hours at various temperatures

6.4. Hardness Altering during Resting

In *Fig. 10.a* and *Fig. 10.b* the evolution of HV is summated after the isochronal heat treatments at various temperatures. The measurements were carried out continuously after resting the samples at room temperature for 0, 0.5, 1.5, 3, 6 hours following the heat treatments. It is clear from the figures that except the sample heated at 150 °C for 1 hour the hardness of the samples being heat-treated for short time (1–6 hours) lowers during a six-hour-period resting at room temperature. It may refer to a small reversible part of a structural relaxation, which is very inter-

esting especially by amorphous alloys. On the other hand, the HV increases during the resting time, when T_a exceeds the 250 °C and the time of heat treatments was longer than 6 hours.

The same can be observed on the samples that were cooled in fluid N_2. The ones being heat-treated before at lower temperature than 250 °C have lower HV than in the a.q. state. The others have higher HV.

6.5. Electrical Resistance

Fig. 11.a–11.f show the change of the relative electrical resistivity (R/R_0, R_0 measured at −196 °C) of the samples heat treated at various temperatures for various times over the temperature interval −196 – +5 °C. As one can see there is a significant difference between the temperature dependence of R/R_0 on the thermal history of the samples. The R/R_0 of samples annealed for short time is nearly linear. On the contrary the samples being annealed for 6–24 hours exhibit a break of R/R_0 at around −100 °C. This break divides the curve into a 'low' and a 'high' temperature part having different slopes. TCR is lower in the low temperature range.

Some of the results are considerably fluctuating with increasing tendency especially by the samples heat treated for 4 and 6 hours. Because this deviation is obviously larger than the measuring accuracy, its origin cannot be a technical artifact.

7. Discussion

In agreement with the general findings in the literature, a global increase of microhardness and tensile strength and a marked drop of flexibility were observed during the isothermal heat treatments.

These changes are the consequence of structural relaxation during which topological and chemical reordering are taking place in the glassy state. As a result of the reordering, the covalent bonding character (introduced by the glass former metalloids) is increasing. This manifests itself in the hardness increase and, also in the brake down of flexibility.

In spite of the observed property changes caused by the long time annealing (structural relaxation) the applicability of the investigated $Fe_{40}Ni_{40}Si_6B_{14}$ glass as defrosting heating elements is obvious. Though the flexibility (see *Fig. 6, 8*) drops markedly during this heat treatments, the residual flexibility is still sufficient to endure the flexural stresses arising from the cyclic dilatation and contraction during the repeated heating and cooling cycles associated with the working conditions.

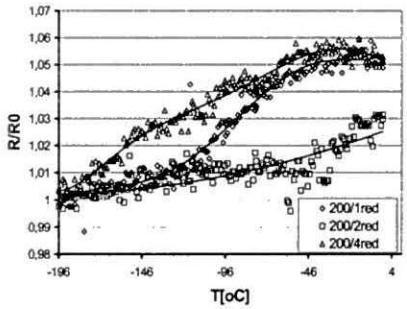

Fig. 11.a. R/R_0 of $Fe_{40}Ni_{40}Si_6B_{14}$ glassy ribbons treated at 200 °C for 1, 2, 4 hours

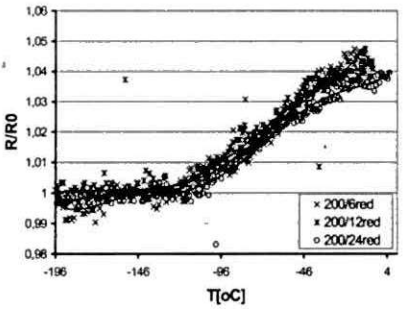

Fig. 11.b. R/R_0 of $Fe_{40}Ni_{40}Si_6B_{14}$ glassy ribbons treated at 200 °C for 6, 12, 24 hours

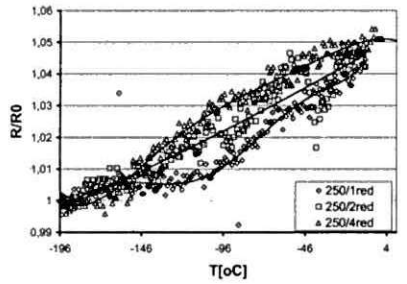

Fig. 11.c. R/R_0 of $Fe_{40}Ni_{40}Si_6B_{14}$ glassy ribbons treated at 250 °C for 1, 2, 4 hours

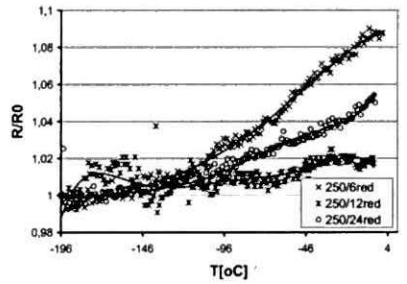

Fig. 11.d. R/R_0 of $Fe_{40}Ni_{40}Si_6B_{14}$ glassy ribbons treated at 250 °C for 6, 12, 24 hours

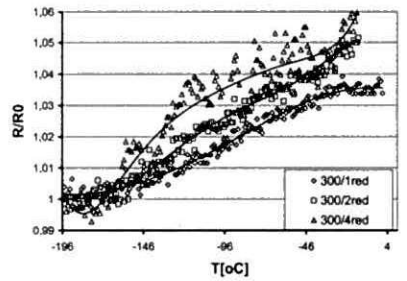

Fig. 11.e. R/R_0 of $Fe_{40}Ni_{40}Si_6B_{14}$ glassy ribbons treated at 300 °C for 1, 2, 4 hours

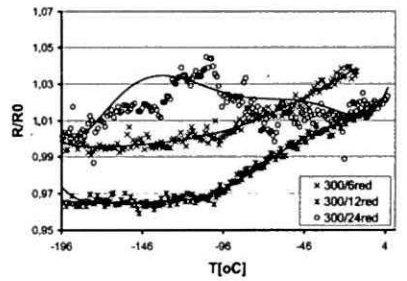

Fig. 11.f. R/R_0 of $Fe_{40}Ni_{40}Si_6B_{14}$ glassy ribbons treated at 300 °C for 6, 12, 24 hours

Disregarding the outlined technical considerations, unknown mechanical prop-

erty changes have been discovered investigating the first period of structural relaxation of this glass. It is obvious, that none of the investigated properties does monotony change during the first period of heat treatments. Comparing the observed phenomena with the similar fluctuations of the amorphous Curie temperature (T_c^{am}) during the same type of heat treatments one can suspect the existence of a hidden dynamic effect taking place either at room or even at low temperatures (−196 °C) in these glasses.

Especially remarkable is, that a definite, transient 'relaxation softening' (hardness decrease and flexibility increase) occur during a certain period of heat treatments (low temperature relaxation, see *Fig. 7*). Another interesting finding of our experiments is the existence of an 'indefinite scattering' and an apparent 'time dependence' of the HV values while resting the samples at room temperature after a certain heat treatment period.

It is also surprising, that HV values during the structural relaxation (as the result of indefinite fluctuations) can be even higher than that for the saturation HV value near the crystalline state, indicating the possible contribution of macroscopic stress-accumulation to the evaluation of HV. This is analogous to the building of the Guinier-Preston zones in certain crystalline metals prior to the appearance of the critical nuclei of the new phases. According to the traditional thermodynamical interpretation of structural relaxation, the process as a whole, can be divided into an irreversible and reversible part. After a certain degree of an irreversible process (caused by an isothermal heat treatment) the structure is supposed to reach an internal equilibrium. Consequently, at the resting temperature, which is significantly lower than the equilibration temperature, the sample should be stable from any point of view of properties. Consequently, all kinds of 'dynamic effect' in such property changes are surprising, and the complete understanding needs more experimental effort and interpretation as well.

The change in the TCR due to the relaxation heat treatments is also surprising on the basis of the known literature. Originally, the character of TCR (existence of a minimum in the low temperature range etc.) is considered to be dominantly composition dependent. In contrast, we found that the TCR depends strongly on the thermal history. A nearly linear temperature dependence was found at short time annealed samples while TCR of long time annealed samples exhibit a firm brake point, independent form the heat treatment temperature. The slope of TCR versus temperature is different below and above the break point temperature. This ambivalent character hints to the existence of two different CSRO or TSRO in the glass induced by the heat treatments. To clarify the reasons of this behaviour more and detailer investigations are necessary.

8. Conclusion

The main technically relevant result of our investigations is that the mechanical and electrical properties of $Fe_{40}Ni_{40}Si_6B_{14}$ glassy alloy do not change much over the

temperature range of the application and its use as a heating element of a resistivity heating would be impossible. Moreover, the complete understanding of the property change of $Fe_{40}Ni_{40}Si_6B_{14}$is possible only by performing new investigations.

Acknowledgement

Thanks to Prof. J. Bicsák for supplying the micrographs taken from the fractured ribbon cross sections and to J. Tóth for his kind help in the electrical property measurements.

This work has been supported by the Hungarian Research Fund (OTKA) through grants No: T-032739 and No: T-035278.

References

[1] JONES, H., Rapid Solidification of Metals and Alloys, *The Institution of Metallurgists*, ISBN 0901-462-18-7.

[2] LOVAS, A., Az ötvözés és az előállítási körülmények szerepe a vas-bór alapú fémüvegek tulajdonságainak alakításában, kandidátusi értekezés, KFKI, 1990, Budapest.

[3] FARKAS, J. – KISS, L. – LOVAS, A. – KOVÁCS, P. – GÉCZI, E., Electrochemical Corrosion of $Fe_{1-x}B_x$ Metallic Glasses, *Conference on Metallic Glasses: Science and Technology*, Budapest 1980.

[4] HASIMOTO, K., Chemical Properties in: *Butterworth Monographs in Materials, Amorphous Metallic Alloys*, edited by F. E. Luborsky.

[5] GULYÁS, CS., Konstruktion eines Curiepunktschalters, mit Verwendung von Glasmetallen, *47. Internationales Wissenschaftliches Kolloquium*, Technische Universität Ilmenau, 2002.

[6] CHEN, H. S., Structural Relaxation in Metallic Glasses, in: *Butterworth Monographs in Materials, Amorphous Metallic Alloys*, edited by F. E. Luborsky.

[7] BÖHÖNYEY, A. – KISS, L. F. – GULYÁS, CS. – TICHY, G., Reversible Curie-Point Relaxation in FeNiB and FeNiP Amorphous Alloys, *SMM 16 Conference*, Düsseldorf 2003.

[8] O'NEILL, H., *Hardness Measurements of Metals and Alloy*, Chapman and Hall, London, 1967.

[9] LOVAS, A. – KISS, L. F. – SOMMER, F., Hardness and Thermal Stability of Fe-Cr-Metalloid Glasses, *Journal of Non-Crystalline Solids*, Elsevier Science B. V., 1995, pp. 608–611.

[10] NAKA, M. – TOMIZAWA, S. – MASUMOTO, T. – WATANABE, T., Effects of Alloying Elements on Strength and Thermal Stability of Amorphous Iron-Base Alloys, in *Rapidly Quenched Metals II*, ed. N. J. Grant and B. C. Giessen, Vol. 1, MIT, Boston, MA, 1976.

[11] LOVAS, A. – KISDI-KOSZÓ, É. – KONCZOS, G. – POTOCKY, L. – VÉRTESY, G., Casting of Ferromagnetic Amorphous Ribbons for Electronic and Electrotechnical Applications, *Philosophical Magazine B*, **61** (1990), pp. 579–565.

[12] KOVÁCS, I. – LENDVAI, J., The Mechanical Properties of Metallic Glasses, Institute for General Physics at Loránd Eötvös University, Budapest.

[13] SPAEPEN F., *Acta Met.*, **25** (1977).

[14] ADAM, A. – GIBBS, J. H., *J. Chem. Phys.*, **43** (1965).

[15] DUWEZ, *Trans. Amer. Soc. Metals*, **60** (1967), pp. 607–633.

[16] NAGEL, S. R., Electronic Structure and Transport Properties of Metallic Glasses, *Conference on Metallic Glasses: Science and Technology*, Budapest 1980.

[17] LOVAS, A. – KISDI-KOSZÓ, E. – POTOCKY, L. – NOVÁK, L., *J. Mater. Sci.*, **22** (1987), pp. 1535–1646.

[18] KÖSTER, U. H. – HILLENBRAND, G., Mechanical Properties of Amorphous Alloys, *Conference on Metallic Glasses: Science and Technology*, Budapest, 1980.

[19] GULYÁS, CS., Thesis work, *Budapest University of Technology and Economics, Faculty of Transportation Engineering, Department of Vehicles Manufacturing and Repairing*, Budapest, 2001.

[20] BÁN, K. – KOVAC, J. – NOVAK, L. – LOVAS, A., New Effects in Amorphous Curie-Temperature Relaxation, in *Acta Electrotechnica et Informatica* **2** No. 3 (2002), Kosice, Slovak Republic, 2002, ISSN: 1335-8243.

[21] STUBICAR, M., Microhardness Characterization of Stability of Fe-Ni Based Metallic Glasses, *J. Mat. Sci.*, **14**, Chapman and Hall Ltd., Great Britain, 1979.

[22] GULYÁS, CS. – PÁL, Z. – LOVAS, A., The Evolution of Microhardness and Flexural Strength in $Fe_{40}Ni_{40}Si_6B_{14}$ Glassy Alloys During Structural Relaxation, *Advanced Manufactoring And Repair Technologies In Vehicle Industry*, Zilina, 2003.